Negative Barkhausen jumps in permalloy thin-film microstructures

Shuqiang Yang, G. S. D. Beach, and J. L. Erskine[a)]
Department of Physics, The University of Texas at Austin, Austin, Texas 78712

(Received 18 August 2006; accepted 29 September 2006; published online 15 December 2006)

Dual-beam high-resolution magneto-optic Kerr effect polarimetry and magnetic force microscopy (MFM) are used to study Barkhausen jumps in thin-film permalloy microstructures. Negative jumps (changes in local magnetization that oppose the drive field) are always accompanied by a nearly simultaneous positive jump, and the power-law dependence of jump-size statistical distributions of positive and negative jumps are similar. These observations, supported by sequential MFM domain images taken during field-driven reversal, indicate that negative jumps are driven by configurational changes of local domain structure associated with positive jumps that are governed by pinning, exchange, and anisotropy energies. The eddy-current coupling mechanism, that appears to account for negative jumps in bulk materials, is suppressed by sample thickness scaling in the thin-film microstructures. © *2006 American Institute of Physics*. [DOI: 10.1063/1.2400513]

INTRODUCTION

The random changes in local magnetization resulting from domain-wall depinning under field-driven magnetization reversal are known as the Barkhausen effect[1]. Since their discovery, Barkhausen effects have been extensively studied[2] because they belong to an important class of nonlinear-dynamical phenomena that exhibit power-law distributions of jump sizes and durations characteristic of scale-invariant behavior.[3,4] The universal stochastic behavior observed in low sweep-rate magnetic reversal can provide insight into related behavior associated with stock market fluctuations, earthquakes, material failure by fracture, and other related phenomena.

In all Barkhausen jumps, the magnetic system experiences a transition between two different metastable states separated by an energy barrier. Most Barkhausen jumps (positive jumps) produce changes in local averaged magnetization that reduce the Zeeman energy $\langle M \cdot H \rangle_v$ within the jump volume, where the brackets represent an average of the scalar product of magnetization M and local magnetic field H over the jump volume. A succession of such jumps can eventually result in field-driven magnetization reversal. Negative Barkhausen jumps,[5] in which changes in local magnetization oppose the applied field direction, have also been detected in several bulk materials using standard pickup coil technology[6–8] and, more recently, high-resolution magneto-optic techniques.[9] Negative Barkhausen jumps require a source of energy sufficient to overcome not only the local pinning potential, but also the increase in local Zeeman energy associated with the new local magnetic configuration that has magnetization opposing the applied field.

One source of energy that can drive negative Barkhausen jumps is thermal energy. A thermally excited fluctuation in local magnetization can occur when thermal energy is comparable to the change in magnetic energy associated with a Barkhausen jump. Thermal effects are justifiably neglected in describing Barkhausen phenomena in bulk materials because the effective (Barkhausen) volumes are too small to produce measurable signals in most types of measurements:[4] the volume is given by

$$(2\mu_0 M_s H_p)\Delta V \sim kT,$$

where H_p is the local pinning field, M_s is the saturation magnetization, T is the temperature, and ΔV is the volume over which the magnetization reverses during a jump. Reasonable assumptions for parameters associated with soft magnetic materials lead to $\Delta V < 10^{-18}$ m^3. Estimates of signals in inductive pickup experiments corresponding to this jump volume fall far below the sensitivity limit of this technique. Thus any negative Barkhausen jumps observed by pickup coil experiments in bulk magnetic materials must result from a mechanism different from thermal excitation.

Negative Barkhausen jumps were predicted in 1930 (Ref. 5) and detected experimentally in 1951.[6] The experimental observation of negative Barkhausen jumps was carried out using a Fe–Si frame monocrystal.[5] This experiment was followed by experiments on annealed polycrystalline wires[8] and amorphous ribbons.[9] Some early work also explored the change in the surface domain structure of polycrystalline Fe–Si specimens by magneto-optic Kerr microscopy.[10] That work provided evidence of field-driven changes in domain configurations that could result in negative Barkhausen jumps.

The physical mechanisms responsible for negative Barkhausen jumps have not been clearly identified by prior work, although the experimental results offer several possibilities. Initial experiments revealed a strong correlation between the jump-size distributions of positive and negative Barkhausen jumps, leading to the conclusion that negative jumps were coupled with, and in some way dependent on, positive jumps. Experiments on polycrystalline samples revealed negative jumps when sufficiently high temporal resolution was used ($\Delta\tau \sim 1\ \mu$s) but failed to detect negative jumps with lower temporal resolution ($\Delta\tau \sim 100\ \mu$s). A model based on local-field coupling induced by eddy-currents[11] from positive jumps yielded estimates of local-

[a)]Electronic mail: erskine@physics.utexas.edu

field amplitudes ($H \sim 5 \times 10^3$ Oe) with rise times ($\tau_r \sim 0.5$ μs) that appear to account for the negative jump observations in bulk materials. Additional tests of the eddy-current coupling model in bulk materials based on the strong temperature dependence of conductivity (and thus eddy-current coupling) were subsequently carried out that provided additional support for this mechanism.[12] The eddy-current model also seems to account for the fact that no negative jumps are observed in high resistivity ferrite materials.[13]

The most recent study of negative Barkhausen jumps compared experimental results obtained from an amorphous Fe–Ni based alloy ribbon ($Fe_{63}B_{14}Si_8Ni_{15}$) using both the traditional inductive pickup coil technique and a new high-spatial resolution magneto-optic Kerr effect (MOKE) polarimeter.[9] Statistical distributions of positive and negative jump amplitudes obtained from the pickup coil measurements (over three-decade dynamic range) and from a 50 μm-resolution magneto-optic investigation (about 1 decade dynamic range) yielded the same (jump amplitude) power-law exponent: $\alpha = 1.6$. This result is a strong indication of scale invariance of both positive and negative Barkhausen jump distribution functions in the amorphous ribbon system, and a good indication that the negative jumps are coupled to positive jumps. Probing the sample surface at 50 μm spatial resolution using the MOKE technique revealed surface regions where negative jumps were produced, and other regions where no negative jumps were produced. One puzzling feature of the inductive pickup data is the appearance of isolated negative Barkhausen jumps that seem to be inconsistent with the eddy-current mechanism, thus suggesting an alternative mechanism may be required to explain all observed negative Barkhausen jump effects.

This paper describes experiments in which negative Barkhausen jumps are studied in thin-film permalloy microstructures. Magnetization reversal was simultaneously probed globally and locally with high temporal resolution using a dual-beam magneto-optic technique. The film thickness is 50 nm, which is thin enough to suppress eddy-current effects (even in high-conductivity materials) due to thickness scaling of these effects.[14,15] The simultaneous measurement of positive and negative Barkhausen jumps at high (≈ 0.1 μs) temporal resolution and sequential magnetic force microscopy (MFM) images of the same microstructure provides the basis for postulating a mechanism for producing negative Barkhausen jumps in thin films (that is also present in bulk materials).

EXPERIMENT

Figure 1 shows a schematic representation of the dual-beam MOKE polarimeter. Two lasers are used: a 45 mW solid-state laser ($\lambda = 658$ nm) and a 20 mW He–Ne laser ($\lambda = 632.8$ nm). Each laser is part of a separate high-sensitivity, high-spatial resolution polarimeter similar to the instrument (previously described)[16] that was used to study domain-wall dynamics and Barkhausen effects in permalloy microstructures. Beam expanders, objective lenses, and other optics allow the two beams to be focused on the microstructured sample with overlapping but independently selected spot

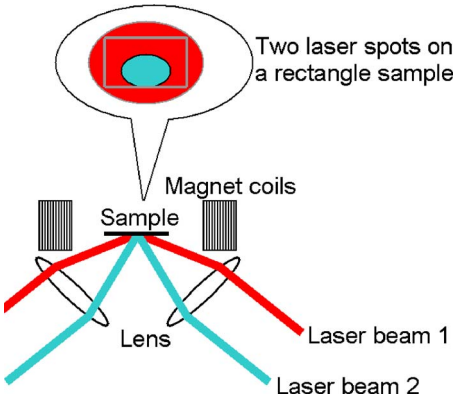

FIG. 1. (Color online) Schematic diagram of dual-beam MOKE experiment.

sizes. The 45° incident angle provides elliptical beam profiles with minimum spot size (long axis) of 20 μm. Each polarimeter achieved (amplifier bandwidth limited) temporal resolution of approximately 0.1 μs, and a signal-to-noise ratio of approximately 5:1 at a sampling time of 0.1 μs/sample. Slightly higher sensitivity was achieved for the smaller spot channel ($\lambda = 658$) used to probe negative jumps due to its higher laser power. Both polarimeters were configured to measure the longitudinal MOKE which is sensitive to the magnetization parallel to the x-direction applied field (M_x) averaged over the illuminated sample area.

Six rectangular permalloy microstructures were fabricated using standard e-beam lithography/lift-off techniques. Three microstructures were 100×70 μm^2; the other three were 50×36 μm^2. All six structures were fabricated on a thermally oxidized Si(100) substrate. The film (thickness ~ 50 nm) was grown by e-beam evaporation at a pressure of 4×10^{-9} Torr. Sequential MFM images of the microstructure domain patterns were obtained using a Nanoscope IV atomic force microscope (AFM)/MFM with Helmholtz coils adapted to provide a magnetic field. Several dozen MFM images and over 6000 MOKE switching loops were measured in the experiment.

RESULTS AND DISCUSSION

Figure 2 displays typical hysteresis loops measured using the dual-beam MOKE polarimeter. The applied field was

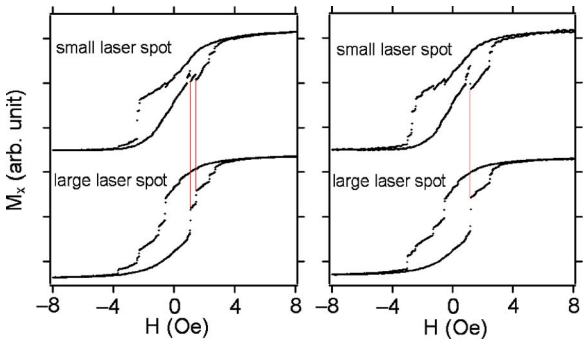

FIG. 2. (Color online) Typical hysteresis loops obtained from large laser spot (full area of microstructure) and small lasers spot (~20% of sample area) showing negative Barkhausen jumps from smaller region correlated with positive Barkhausen jumps from entire sample.

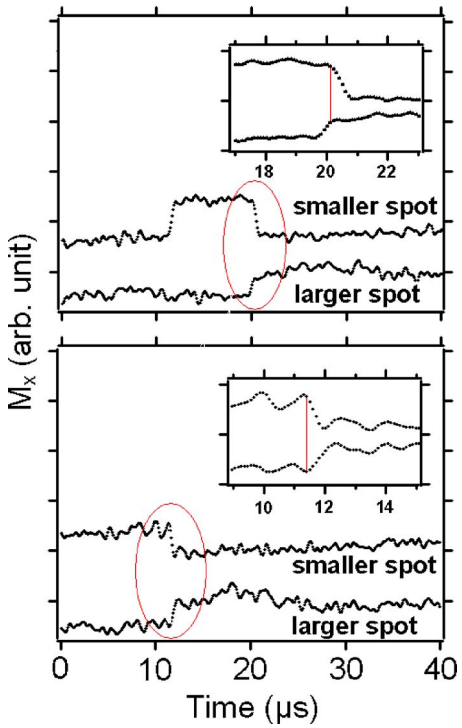

FIG. 3. (Color online) High temporal resolution time record of spatially resolved magnetization from small region (upper traces of both panels) showing negative Barkhausen jumps correlated with positive Barkhausen jumps from full area of microstructure. Each point corresponds to a 0.1 μs sample. Upper panel with expanded-scale insert shows negative jump occurring at the end of positive jump (time delay approximately 0.5 μs). Lower panel shows negative jump occurring at leading edge of positive jump (no time delay).

a linear ramp (triangle wave) at a frequency of 1.25 Hz. The effective sampling time for data presented in Fig. 2 was 0.5 ms (each loop contains 1600 points) which accounts for the high signal-to-noise ratio. The upper panels correspond to the smaller-diameter beam (20 μm); the lower panels correspond to the larger-diameter beam (the larger-beam diameter $1/e$ width was adjusted to be approximately equal to the microstructure width). Therefore, the larger beam probed all Barkhausen jumps produced by the microstructure within the sensitivity limit; the smaller beam probed below 20% of the microstructure area. Analysis of over 6000 dual-beam hysteresis loops resulted in the following qualitative characteristics of positive and negative Barkhausen events in the thin-film permalloy microstructures: (1) negative jumps were observed only in the smaller spot channel; (2) every negative jump was correlated with a positive jump; (3) all negative jumps were smaller than the corresponding positive jumps; (4) negative jumps occurred at a rate of approximately 20% of positive jump production, and the rate of negative jump production was sensitive to the location of the smaller beam on the sample.

Figure 3 displays portions of a dual-channel magnetization measurement at high temporal resolution (0.1 μs/sample). The instrumentation noise floor is apparent at the short integration time interval [compare noise of $M_x(t)$ data in Figs. 2 and 3]. Barkhausen jumps are clearly resolved, and the specific events displayed in the two panels were selected to demonstrate evidence of measurable time delays in the jump dynamics. The lower panel corresponds to an event where the positive jump and negative jump occur simultaneously within the temporal resolution of the measurement. The upper panel corresponds to an event where the negative jump is not triggered until after most of the ΔM associated with the positive jump has occurred (a 0.5 μs delay). The upper panel also shows an event in which the negative jump was preceded by a positive jump (10 μs). The difference in sensitivity of the two channels resulting from the difference in probed area results in the amplitude of the positive jump in the large beam area channel being obscured by the noise floor.

Time delays of several tenths of a microsecond [as shown in Fig. 3(a)] can be reconciled with the proposed mechanism for negative-Barkhausen jump production based on field-driven configurational changes in domain patterns and the domain-wall velocities associated with wall displacement. Jump-size distributions are discussed later (Fig. 4). Positive jump sizes range from values corresponding to approximately half of the total sample volume to below the sensitivity limit; the largest negative jump sizes are at least a factor of 10 smaller. Typical domain-wall velocities can be estimated from the fractional change in magnetization of a positive jump and the time required for the jump to occur as described previously.[16] Typical domain-wall velocities during a Barkhausen jump are $v \sim 50$ m/s, and typical jump execution times (Fig. 3) are $\Delta\tau \sim 1$ μs (for a large jump). Negative jump time delays of several tenths of a microsecond to a microsecond following the initiation of a positive jump can be accounted for based on the jump execution time. If a negative jump event is stimulated at the initial location of a domain wall that produces a positive jump, the negative jump will be simultaneous with the positive jump. However, if the negative jump results from a configurational change of the domain structure that is not stimulated until near the end of a positive jump, there must be a time delay equal to the positive jump execution time which is subject to the domain-wall velocity and jump size.

Figure 4 displays log-log plots of probability distributions as a function of jump size for positive and negative Barkhausen jumps. Both distributions manifest cutoff behavior associated with the sample size (large beam, positive jumps) or the beam size (small beam, negative jumps) as well as structure for large jump amplitudes attributed to the relatively small number of domain configurations that can be achieved in a microstructured thin-film sample (breakdown of power-law scaling resulting from finite size effects).[17,18] Jump-size distributions for smaller values of ΔM_x (for both positive and negative jumps) show evidence of the uniform power-law scaling observed in jump-size probability distributions in bulk[4] and larger area thin-film samples.[9] The straight lines in Fig. 4 correspond to power-law fits in the small jump-size regions, where finite-size effects do not disrupt the power-law behavior. The positive and negative jump-size distributions are very similar in this region, and are described by scaling exponents of 1.45 and 1.47, respectively. This observation suggests a correlation between the two processes.

Figure 5 displays a sequence of MFM domain images

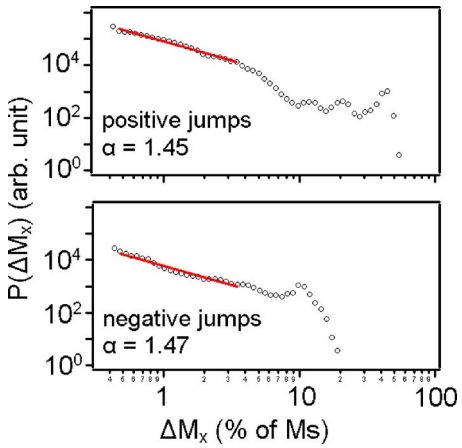

FIG. 4. (Color online) Log-log plots of probability distribution $P(\Delta M_x)$ vs jump size ΔM_x for positive and negative Barkhausen jumps. The unit of ΔM_x is percent of saturation magnetization of the sample. Cutoff behavior and nonuniform power-law scaling of large ΔM_x result from relatively small numbers of allowed domain configurations; at smaller ΔM_x scales, both positive and negative distributions exhibit power-law behavior characterized similar exponents (straight line).

obtained during a slow linear-ramp-driven magnetization reversal cycle of one of the microstructures. Drawings that show more clearly the location of domain walls are presented to the right with an elliptical outline that simulates a possible location of a local MOKE probe. Suggested spin directions corresponding to the various domains are indicated in the schematic drawing. The dotted lines indicate cross-tie structures.[19,20] The lower panel displays $\langle M_x \rangle$ obtained by numerical averaging of the entire sample and $\langle M_x \rangle$ for the elliptical region, simulating a dual-beam measurement of the spatially resolved magnetization of the three domain configurations. This simulation of a dual-beam MOKE measurement demonstrates how a configurational change of domain structure probed at a selected region of an actual microstructured sample can manifest a negative Barkhausen jump (small region) resulting from a larger (full sample) positive jump.

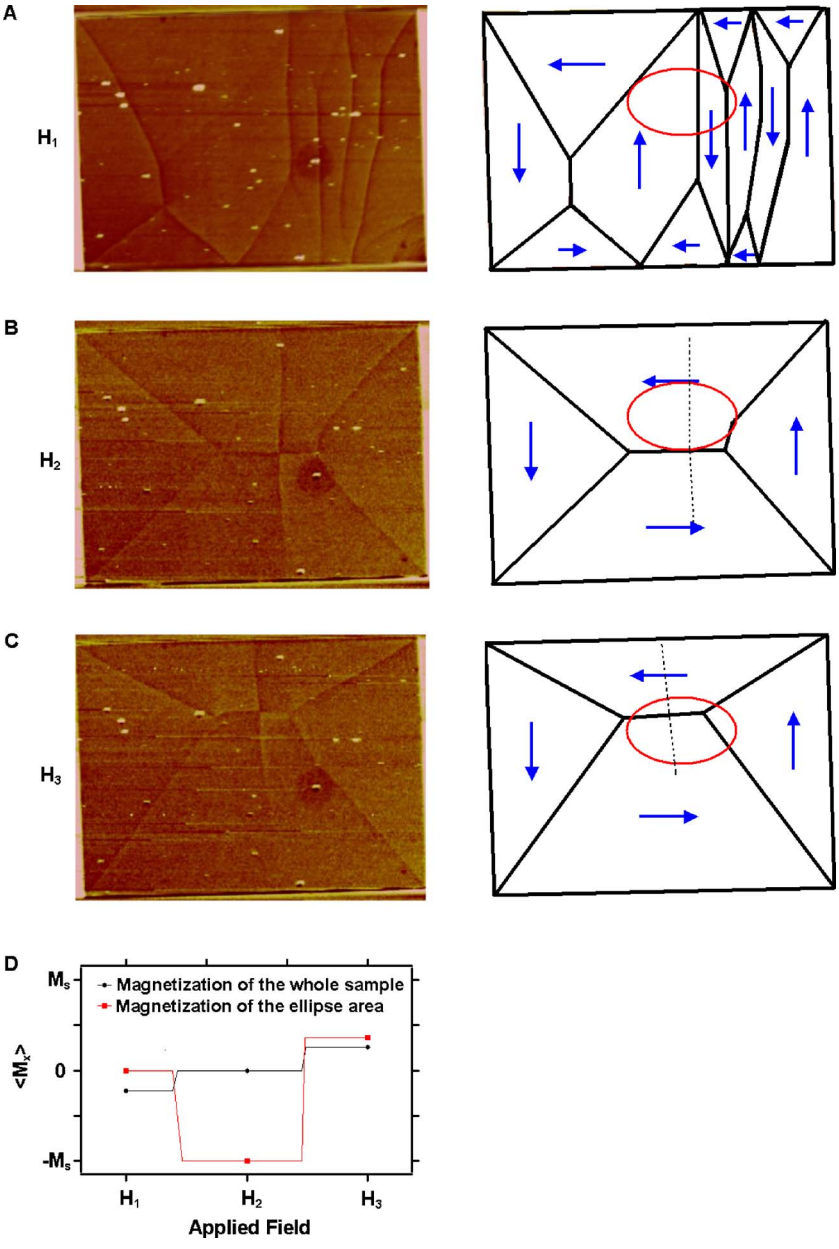

FIG. 5. (Color online) Three left-side panels: sequential MFM images of microstructure domain walls as applied magnetic field is increased in discrete increments. Three right-side panels: schematic diagrams of MFM images with suggested spin orientation within each domain. Ellipse represents a region of the sample that, if probed by the dual-beam MOKE polarimeter, would yield a negative Barkhausen jump between panels A and B. Dotted lines indicate cross-tie structure. Lower panel: magnetization of entire sample (square) and of region enclosed in ellipse (circle), (as fraction of M_s enclosed in areas) obtained by numerical average of M_x over the spin configurations. The red curve shows a negative Barkhausen jump between the H_1 and H_2 domain configurations.

CONCLUSIONS

Negative Barkhausen jumps are studied in thin-film permalloy microstructures. The films are thin enough to suppress eddy-current effects and the measured

Barkhausen volumes associated with negative jumps are too large to be attributed to thermal excitation effects. A mechanism that is independent of eddy-current and thermal activation effects is proposed to account for the negative Barkhausen jumps: configurational changes in domain-wall patterns in which a positive Barkhausen jump drives a region of the sample in a manner that results in an increase in local magnetization opposed to the drive-field direction. These configurational changes are driven by the Zeeman energy, but require the complicated local pinning potentials and anisotropy energies found in all practical magnetic specimens. Time delays of several tenths of a microsecond are observed in the coupled negative jump dynamics and these are compatible with the measured wall velocities and the feature of the mechanism that allows a negative jump to occur at any time during the driving positive jump event.

ACKNOWLEDGMENTS

This work was supported by NSF (NIRT/DMR-0404252), the Texas Coordinating Board (ATP-0099) and by the Robert A. Welch Foundation. Microstructure fabrication was carried out using facilities of the Center for Nano and Molecular Science and Technology at UT-Austin.

[1] H. Barkhausen, Phys. Z. **20**, 401 (1919).
[2] G. Durin and S. Zapperi, "The Science of Hysteresis," Vol. II, edited by G. Bertotti and I. Mayergoyz (Elsevier, Amsterdam, 2006), pp. 181–267.
[3] J. P. Sethna, K. A. Dahmen, and C. R. Meyers, Nature (London) **410**, 242 (2001).
[4] S. Zapperi, P. C. Izeau, G. Durin, and H. E. Stanley, Phys. Rev. B **58**, 6353 (1998).
[5] A. Zentko and V. Hajko, Czech. J. Phys., Sect. B **B18**, 1026 (1968).
[6] R. Becker, Z. Phys. **62**, 253 (1930).
[7] L. V. Kirensky and W. F. Ivlev, Dokl. Akad. Nauk SSSR **76**, 389 (1951). [Sov. Phys. Dokl. **1**, 1 (1956)].
[8] V. Hajko, A. Zentko, and S. Filka, Czech. J. Phys., Sect. B **19**, 547 (1969).
[9] M. Zani and E. Puppin, J. Appl. Phys. **94**, 5901 (2003).
[10] J. Kranz and A. Schauer, Ann. Phys. **7**, 84 (1959).
[11] A. Zentkova, A. Zentko, and V. Hajko, Czech. J. Phys., Sect. B **B19**, 547 (1969).
[12] This experiment was alluded to in Ref. 11.
[13] A. Zentkova, Czech. J. Phys., Sect. B **B19**, 1454 (1969).
[14] H. J. Williams, W. Shockley, and C. Kittel, Phys. Rev. **80**, 1090 (1950).
[15] C. Nistor, E. Faraggi, and J. L. Erskine, Phys. Rev. B **72**, 014404 (2005).
[16] S. Yang and J. L. Erskine, Phys. Rev. B **72**, 064433 (2005).
[17] E. Puppin, Phys. Rev. Lett. **84**, 5415 (2000).
[18] E. Puppin, S. Ricci, and L. Callegaro, Appl. Phys. Lett. **76**, 2418 (2000).
[19] R. D. Gomez, T. V. Luu, A. D. Pak, I. D. Mayergoyz, K. J. Kirk, and J. N. Chapman, J. Appl. Phys. **85**, 4598 (1999).
[20] M. Bartheimess, C. Pels, A. Thieme, and G. Meier, J. Appl. Phys. **95**, 5641 (2004).